3 Waves with dielectric boundaries

3.1 REFLECTION OF WAVES BY A DIELECTRIC BOUNDARY

In Section 1.9 we saw that when waves encounter a boundary there are, in general, both reflected and transmitted waves. This is in accord with the everyday experience that sunlight is partly reflected and partly transmitted by a window. Engineers commonly speak of the transmission loss and return loss which are expressed in decibels as

$$\text{Transmission loss} = -10 \log_{10} \left| \frac{\boldsymbol{S}_t}{\boldsymbol{S}_i} \right| \tag{3.1}$$

and

$$\text{Return loss} = -10 \log_{10} \left| \frac{\boldsymbol{S}_r}{\boldsymbol{S}_i} \right| \tag{3.2}$$

where $\boldsymbol{S}_i$, $\boldsymbol{S}_t$ and $\boldsymbol{S}_r$ are the Poynting vectors of the incident, transmitted and reflected waves. The Poynting vector in a lossless dielectric material is related to the electric field strength and the wave impedance by

$$|\boldsymbol{S}| = \frac{1}{2}|\boldsymbol{E}|^2/Z_w = \frac{1}{2}\sqrt{\left(\frac{\varepsilon}{\mu}\right)}\,|\boldsymbol{E}|^2. \tag{3.3}$$

For the case of normal incidence on a dielectric surface the amplitudes of the transmitted and reflected waves can be calculated from (1.84) and (1.85) with the results

$$\frac{E_t}{E_i} = \frac{2\sqrt{\varepsilon_1}}{\sqrt{\varepsilon_1} + \sqrt{\varepsilon_2}}$$
$$\frac{E_r}{E_i} = \frac{\sqrt{\varepsilon_1} - \sqrt{\varepsilon_2}}{\sqrt{\varepsilon_1} + \sqrt{\varepsilon_2}}. \tag{3.4}$$

The permeabilities of all dielectric materials are equal to μ_0 to engineering accuracies so they cancel out of the equations. It is evident that both the wave amplitudes are non-zero except for the trivial case when $\varepsilon_1 = \varepsilon_2$.

3.2 TOTAL INTERNAL REFLECTION

The position is rather different when the angle of incidence is not zero. Equation (1.90) shows that if the permeabilities are assumed to be equal then

$$\sin\theta_2 = \sqrt{\left(\frac{\varepsilon_1}{\varepsilon_2}\right)}\sin\theta_1. \tag{3.5}$$

If ε_1 is greater than ε_2 then there will be a critical value of θ_1 such that $\sin\theta_2 = 1$. For angles of incidence larger than this the wave must be totally reflected. This phenomenon is sometimes observed in underwater photographs where the water surface appears to be a mirror. It has important applications in optical fibres to which we shall return later. At a more mundane level it is employed in the edge-lit signs sometimes seen in cinemas. For the interface between glass and air the critical angle is around 42°.

The phenomenon can also be explained by making use of the concept of wave impedance. From (1.84) and (1.94) the reflected wave amplitude is given by

$$\frac{E_r}{E_i} = \frac{\sqrt{\varepsilon_1}\cos\theta_2 - \sqrt{\varepsilon_2}\cos\theta_1}{\sqrt{\varepsilon_1}\cos\theta_2 + \sqrt{\varepsilon_2}\cos\theta_1} \tag{3.6}$$

when the magnetic field vectors are parallel to the surface. Clearly $|\boldsymbol{E}_r| = |\boldsymbol{E}_i|$ when $\theta_2 = 90°$. Z_{n2} is then zero so this case corresponds to the termination of a transmission line by a short circuit. If the wave is polarized with the electric field vector parallel to the surface we obtain

$$\frac{E_r}{E_i} = \frac{\sqrt{\varepsilon_1}\cos\theta_1 - \sqrt{\varepsilon_2}\cos\theta_2}{\sqrt{\varepsilon_1}\cos\theta_1 + \sqrt{\varepsilon_2}\cos\theta_2} \tag{3.7}$$

using (1.97) and the conclusion is the same except that Z_{n2} is now infinite corresponding to an open-circuit termination.

An alternative, physical, explanation can be obtained by considering Fig. 1.8. If ε_1 is greater than ε_2 the wave is refracted away from the normal. The limit of this process is reached when the refracted wave is moving parallel to the boundary as shown in Fig. 3.1. For angles of incidence greater than the critical angle the separation of the points A and B is less than the wavelength in region 2 and the boundary conditions cannot be satisfied by a propagating wave. Nevertheless the fields in this region must satisfy the wave equation (2.4). Assuming that the fields vary only with y, z and t then, from (2.27)

$$E = E_2 \exp \mathrm{j}(\omega t - k_y y - k_z z) \tag{3.8}$$

and, substituting this into (2.4) we get

$$k_y^2 + k_z^2 = k_2^2, \tag{3.9}$$

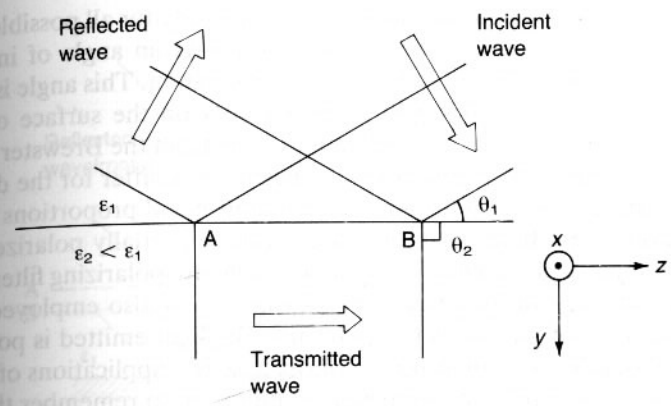

Fig. 3.1 Geometry for total internal reflection of a wave by a boundary between two dielectric materials.

where k_2 is the propagation constant in region 2. If $k_2 < k_z$ then k_y must be imaginary so that the wave decays exponentially away from the boundary. A wave of this kind is called an evanescent wave.

3.3 THE BREWSTER ANGLE

From (3.6) and (3.7) it appears that there could be conditions under which there is no reflection. Taking (3.7) first the condition is

$$\frac{\cos\theta_2}{\cos\theta_1} = \sqrt{\left(\frac{\varepsilon_1}{\varepsilon_2}\right)}. \tag{3.10}$$

If $\varepsilon_2 > \varepsilon_1$ then $\theta_2 > \theta_1$ from (3.10) and $\theta_2 < \theta_1$ from (3.5). These conclusions are contradictory so the condition can never be satisfied. In the other case when the magnetic field is parallel to the boundary we get

$$\frac{\cos\theta_2}{\cos\theta_1} = \sqrt{\left(\frac{\varepsilon_2}{\varepsilon_1}\right)} \tag{3.11}$$

and this time there is no contradiction. From (3.5) and (3.11)

$$\sin^2\theta_2 + \cos^2\theta_2 = \frac{\varepsilon_1}{\varepsilon_2}\sin^2\theta_1 + \frac{\varepsilon_2}{\varepsilon_1}\cos^2\theta_1 \tag{3.12}$$

or

$$1 = \left[\frac{\varepsilon_1}{\varepsilon_2} - \frac{\varepsilon_2}{\varepsilon_1}\right]\sin^2\theta_1 + \frac{\varepsilon_2}{\varepsilon_1} \tag{3.13}$$

which yields

$$\sin^2\theta_1 = \frac{1}{1 + \varepsilon_1/\varepsilon_2}. \tag{3.14}$$

The right-hand side of this equation is less than unity for all possible values of the permittivities and therefore there is always an angle of incidence which produces no reflected wave for this polarization. This angle is known as the Brewster angle. For light in air incident on the surface of water ($\varepsilon_r = 81$) the angle is 83.7°. Even at angles away from the Brewster angle it is to be expected that the reflection coefficients will differ for the different polarizations. If the incident radiation contains equal proportions of both polarizations then the reflected radiation will be partially polarized. This phenomenon is exploited by photographers who use polarizing filters to cut down the intensity of light reflected off water. It is also employed in the output windows of gas lasers to ensure that the light emitted is polarized.

Throughout this section examples of the practical applications of phenomena have been drawn from optics. It is important to remember that they apply equally to the remainder of the electromagnetic spectrum.

3.4 DIELECTRIC WAVEGUIDES

The property of total internal reflection at an interface between two dielectric materials suggests the possibility of using strips or rods to guide waves in a manner similar to the metallic waveguides discussed in the last chapter. There are, however, important differences between the two cases as we shall see. When a wave is reflected from a metal surface the phase change is independent of the angle of incidence. This is no longer the case for total internal reflection from a dielectric boundary.

To investigate this further let us consider waves whose electric field vectors are parallel to the boundary. The amplitude of the reflected wave is given by (3.7). The angle of refraction can be eliminated by noting that

$$\cos\theta_2 = \pm(1 - \sin^2\theta_2)^{\frac{1}{2}} = \pm\left(1 - \frac{\varepsilon_1}{\varepsilon_2}\sin^2\theta_1\right)^{\frac{1}{2}}. \tag{3.15}$$

Now the wave in region 2 propagates in the direction normal to the boundary as $\exp -jk_2\cos\theta_2 y$. When the angle of incidence exceeds the critical angle the second term on the right hand side of this equation must be greater than unity. $\cos\theta_2$ is then imaginary and the wave decays exponentially with distance from the boundary. Thus it is the negative sign in (3.15) which has physical significance.

Substituting this into (3.7) gives

$$\frac{E_r}{E_i} = \frac{\cos\theta_1 + j(\sin^2\theta_1 - \varepsilon_2/\varepsilon_1)^{\frac{1}{2}}}{\cos\theta_1 - j(\sin^2\theta_1 - \varepsilon_2/\varepsilon_1)^{\frac{1}{2}}} \tag{3.16}$$

so that the phase of the reflected wave is

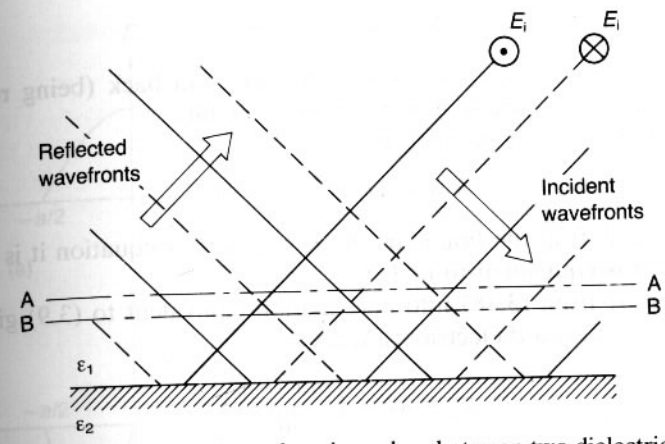

Fig. 3.2 Reflection of plane waves by a boundary between two dielectric materials with the electric field vectors parallel to the boundary.

$$\phi = 2\tan^{-1}\left[\frac{(\sin^2\theta_1 - \varepsilon_2/\varepsilon_1)^{\frac{1}{2}}}{\cos\theta_1}\right] \tag{3.17}$$

relative to the incident wave.

Now consider the interference between plane waves reflected by a dielectric boundary as shown in Fig. 3.2. This figure differs from Fig. 2.5 in that the phase difference between the incident and reflected waves at the boundary is no longer 180°. Within the interference pattern of the waves there are other planes such as A–A on which the phase difference is also ϕ. There are also planes such as B–B on which the phase difference is $-\phi$. If a second boundary coincides with B–B then the boundary conditions are correct for reflection because the roles of the incident and reflected waves have been exchanged with each other.

Figure 3.3 shows the pattern of waves within a dielectric slab of thickness d. The condition for such a pattern to exist is

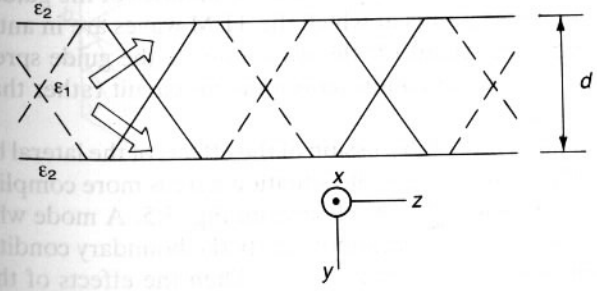

Fig. 3.3 Propagation of waves within a dielectric slab.

$$2k_y d + 2\phi = 2m\pi \tag{3.18}$$

that is, a wave which travels across the slab and back (being reflected twice) must travel a whole number of wavelengths.

Equation (3.18) can be written

$$k_1 d \cos\theta = m\pi - \phi. \tag{3.19}$$

If the phase shift at the boundary is set to π in this equation it is easy to show that it is equivalent to (2.15).

Substituting from (3.18) into an equation equivalent to (3.9) gives the guide equation for a dielectric waveguide

$$k_g^2 = k_1^2 - \left(\frac{m\pi - \phi}{d}\right)^2 \tag{3.20}$$

which can be compared with (2.64). It must be remembered that ϕ is a function of θ_1. At cut-off the angle of incidence is equal to the critical angle so that $\theta_2 = 90°$ in (3.7) and $\phi = 0$ so that

$$k_g = k_1 \sin\theta_1 = k_1 \sqrt{\left(\frac{\varepsilon_2}{\varepsilon_1}\right)} \tag{3.21}$$

and, after a little manipulation the free-space cut-off wavelength is found to be

$$\lambda_c = \frac{2d}{m} \sqrt{\left(\frac{\varepsilon_1}{\varepsilon_0} - \frac{\varepsilon_2}{\varepsilon_0}\right)} \tag{3.22}$$

where $m = 1, 2, 3$, etc.

We see, therefore, that a dielectric slab is capable of supporting a set of modes of propagation very like those in a waveguide. The modes discussed so far are TE modes. Consideration of the other polarity of the waves would lead to TM modes. The difference between the dielectric waveguide modes and those in a metal waveguide is illustrated in Fig. 3.4. In a dielectric guide the waves are not confined to the guide but spread out a little into the surrounding dielectric. The boundaries of the guide therefore lie a little inside those points at which the TEM waves are in antiphase just as shown in Fig. 3.3. At cut-off the wave outside the guide spreads out to infinity so that the cut-off condition is an open-circuit rather than a short-circuit resonance.

We have, so far, avoided discussion of the effects of the lateral boundaries of the guide. The reason is that the situation here is more complicated than it is in metal waveguides. This is clear from Fig. 3.5. A mode which has its electric field in the x direction cannot satisfy the boundary conditions at the dielectric interfaces at $y = 0$ and $y = b$. When the effects of these boundaries are taken into account the patterns of the modes are altered somewhat but the general conclusion that a set of modes of propagation exists is unaffected. If the strip of dielectric is made much wider than its thickness ($b \ll a$) then the theory given above may be expected to be a reasonable approximation.

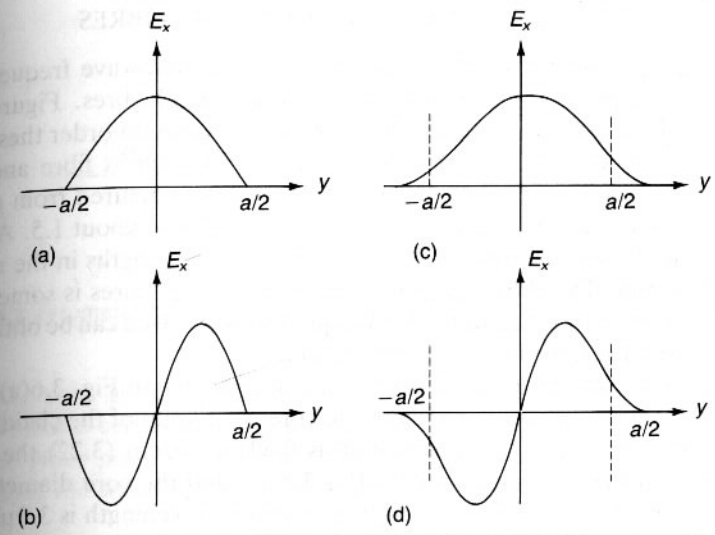

Fig. 3.4 Comparison between TE modes in metal and dielectric waveguides: metal waveguide (a) TE_{01} mode and (c) TE_{02} mode, dielectric waveguide (b) TE_{01} mode and (d) TE_{02} mode.

Dielectric waveguides like that shown in Fig. 3.5 are used in optical integrated circuits and are therefore likely to be of increasing importance.

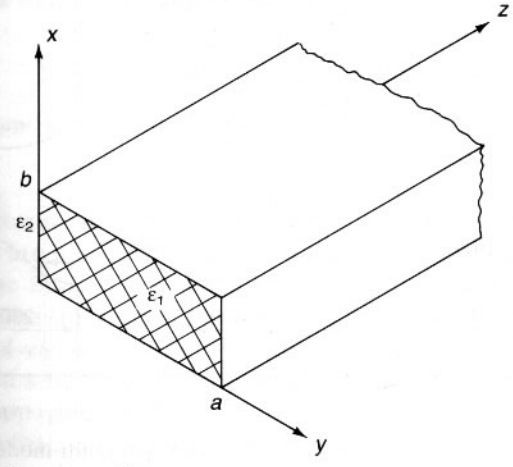

Fig. 3.5 Dielectric waveguide.

3.5 MONO-MODE AND MULTI-MODE OPTICAL FIBRES

Although dielectric guides are sometimes used at microwave frequencies for special purposes the commonest use is in optical fibres. Figure 3.6 shows the three types of fibre which are in common use. In order these are the monomode step-index fibre, the multimode step-index fibre and the multimode graded-index fibre. These fibres are manufactured from glass, silica or plastic with refractive indices in the range 1.0 to about 1.5. At the present time they are normally used with carrier wavelengths in the range 0.82 to 0.85 μm. The theory of propagation in circular fibres is somewhat difficult, but orders of magnitude for the quantities involved can be obtained from the equations in the preceding section.

Consider first the monomode step-index fibre shown in Fig. 3.6(a). Let us assume that the refractive index of the core is 1.5, that of the cladding is 1.4, and that the operating wavelength is 0.82 μm. From (3.22) the core diameter at which this signal is cut off is 1.5 μm and the core diameter at which the next higher mode will propagate at this wavelength is 3.0 μm. It follows that the core diameter must lie somewhere between these limits if only the lowest mode is to propagate. More exact calculations show that the cut-off wavelength of the lowest mode for a circular fibre of diameter d is given by

$$\lambda_c = \frac{\pi d}{2.405} \sqrt{(n_1^2 - n_2^2)}. \tag{3.23}$$

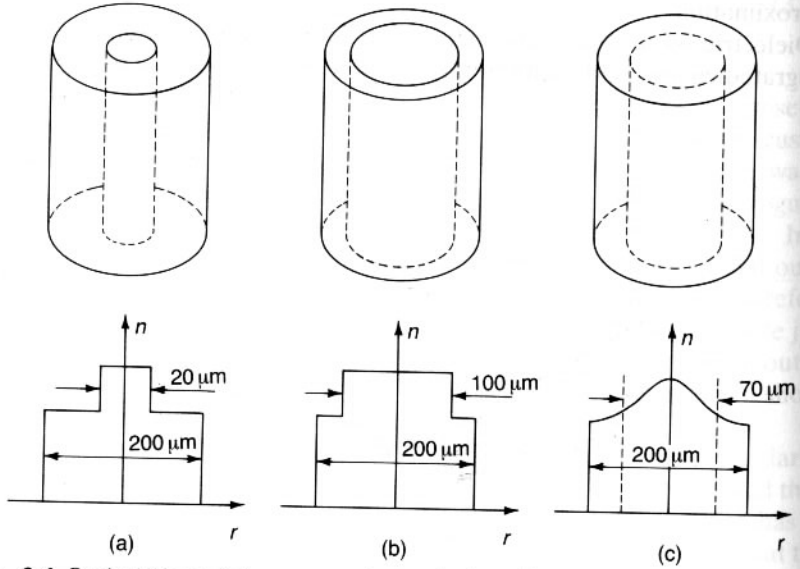

Fig. 3.6 Optical fibres: (a) mono-mode step-index, (b) multi-mode step-index and (c) graded-index fibres.

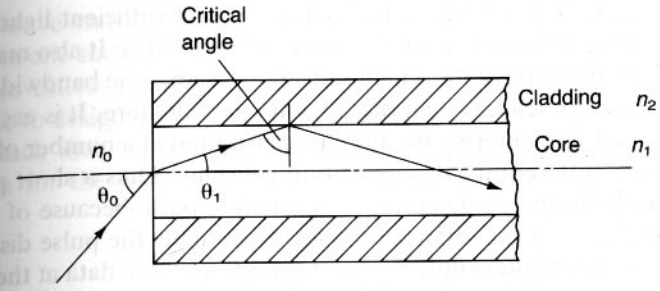

Fig. 3.7 Geometry of light acceptance by an optical fibre.

For the case given above $d = 1.17\,\mu m$ showing that the results of the approximate calculation are not too far from the truth.

The other piece of information which is of interest is the angle of incidence of the wave at the cut-off wavelength. From (3.5) this is

$$\theta = \sin^{-1}\left(\frac{\varepsilon_2}{\varepsilon_1}\right)^{\frac{1}{2}} = \sin^{-1}\left(\frac{n_2}{n_1}\right) \tag{3.24}$$

giving a numerical value of 69° for the fibre described above. This angle is referred to as the critical angle of the fibre. Figure 3.7 illustrates the problem of launching a wave down a monomode step-index fibre. A ray in air is incident on the end of the fibre at an angle θ_0. On entering the core of the fibre it is refracted so that it makes an angle θ_1 with the axis. This angle must be less than 90° minus the critical angle. There is therefore a maximum value of the angle θ_0 for which the incident light will be totally reflected and so captured by the guide. This is known as the maximum acceptance angle θ_m and the cone which it defines is known as the acceptance cone. Another figure of merit which is sometimes used is the numerical aperture defined by

$$\text{NA} = \sin\theta_m. \tag{3.25}$$

It can be shown that

$$\text{NA} = n_1^2 - n_2^2. \tag{3.26}$$

The very small core diameter of a monomode step index fibre means that it is essential to use a laser as the signal source in order to couple sufficient power into the fibre. These fibres have low dispersion and a very wide usable bandwidth (up to 3 GHz km) but are very difficult to splice together. Their principal use is for submarine cables.

If the core of a step-index fibre is made larger then a number of different modes can propagate. Such a fibre is known as a multi-mode step-index fibre (Fig. 3.6(b)). The core diameter is typically one to two orders of magnitude larger than that of the monomode fibres discussed above. This

makes the numerical aperture much larger so that sufficient light can be coupled into the fibre from a light emitting diode (LED). It also makes the splicing of the fibres possible. The disadvantage is that the bandwidth at up to 200 kHz km is much less than that of a monomode fibre. It is easy to see why this is so. Light entering the fibre is transmitted in a number of modes each having a different axial propagation constant. Thus a short pulse of light injected into the guide emerges as a longer pulse because of the different time delays of the different modes. Eventually the pulse dispersion can be so great as to prevent the correct reception of the data at the end of the fibre.

Multi-mode step-index fibres are the cheapest to manufacture. They are in common use for data links of all kinds especially short-distance ones since the bandwidth diminishes with the length of the fibre. For military and avionic systems they have the advantage that they are secure and immune to electromagnetic interference.

The graded-index fibre shown in Fig. 3.6(c) represents a compromise between the two type of fibre already discussed. The core diameter is relatively large so many modes can propagate. The waves are guided by refraction rather than by total internal reflection so the mathematics becomes rather involved. As the refractive index diminishes towards the outside of the fibre a ray making large excursions from the axis tends to spend more time in the low refractive index (high phase velocity) region. This compensates to some extent for the extra path length so that a graded-index fibre is less dispersive than a comparable step-index fibre. Typical bandwidths are from 200 MHz km to 3 GHz km, making this kind of fibre suitable for medium-distance telecommunication links.

3.6 RADOMES, WINDOWS AND OPTICAL BLOOMING

We have noted that there is a close analogy between the propagation of plane waves through different media and the propagation of TEM waves on transmission lines. This analogy enables us to use transmission-line methods for solving plane-wave problems. In particular the half- and

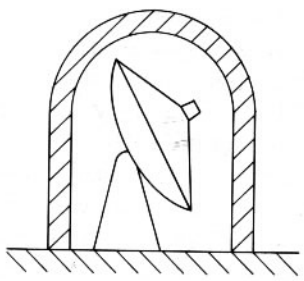

Fig. 3.8 Use of a radome to protect an antenna.

quarter-wave transformers have important practical applications. Figure 3.8 shows one such application. A radar antenna is enclosed by a dielectric enclosure called a radome to protect it from the weather. It is clearly desirable to design the radome in such a way that it does not reflect a lot of power back into the antenna. To investigate this problem we recall the equation for the transformation of impedances on lossless transmission lines

$$\frac{Z_{in}}{Z_0} = \frac{Z_L + jZ_0 \tan kl}{Z_0 + jZ_L \tan kl}. \tag{3.27}$$

This equation gives the input impedance when a line having characteristic impedance Z_0 and electrical length kl is terminated by an impedance Z_L. Making use of the analogy between plane waves and transmission lines we replace the characteristic impedance of the line by the wave impedance of the dielectric and the load impedance by the wave impedance of free space. If the radome is to be matched to the incident wave then the input impedance must also be the wave impedance of free space. The condition for this to occur is $\tan kl = 0$ that is $l = n\pi/2$, where $n = 1, 2, 3$, etc. Thus a sheet of dielectric which is an integral number of half wavelengths thick does not reflect any of the incident wave. Reference to (1.84) shows that this is because the waves reflected from the front and back faces of the sheet are in antiphase and so cancel each other out. In practice the problem is more difficult than this because the radome lies in the near field region of the antenna (see Ch. 5). For further information on radomes see Rudge *et al.* (1982–3).

Example

Find a suitable thickness for a perspex radome to operate at 10 GHz. (ε_r = 2.6 for perspex at 10 GHz).

Solution

At 10 GHz the free-space wavelength is 30 mm so the wavelength in the perspex is $30/\sqrt{2.6} = 18.6$ mm. Possible thicknesses for the radome are therefore 9.3 mm, 18.6 mm, 27.9 mm, etc. The thickness actually used would depend upon the need for adequate strength and rigidity.

The same principle can be used whenever it is necessary to put a dielectric barrier between two regions having the same wave impedance. Thus it can be used to provide pressure-tight windows in waveguides. The disadvantage of the technique is that it is narrow band because a small change of frequency causes the electrical length of the dielectric region to depart from $\lambda/2$.

When the thickness of the dielectric slab is not equal to an exact number

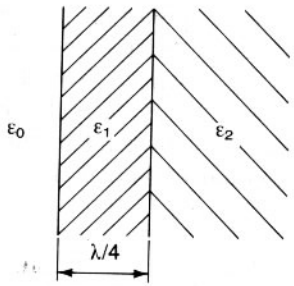

Fig. 3.9 Use of a quarter-wave coating to reduce the reflection coefficient at a dielectric boundary.

of half wavelengths it is still possible to reduce the reflected signal intensity by using the principle of the quarter-wave transformer to match the wave impedance in the dielectric to that of free space. Figure 3.9 shows how this is accomplished. The dielectric slab (permittivity ε_2) is coated with a thin layer of a dielectric of permittivity ε_1. The thickness of this layer must be an odd number of quarter wavelengths, the wavelength, of course, being calculated for the material of the layer. A common application of this technique is in the 'blooming' of lenses for cameras and other optical instruments. The impedances are only matched exactly at one wavelength, but the band of wavelengths in the visible spectrum is less than one octave so the mismatches at the red and blue ends of the spectrum are not too serious if the system is designed at the centre frequency. Blooming is achieved by vacuum deposition of materials such as magnesium fluoride ($n = 1.38$) and cryolite ($n = 1.36$) on the surface of the glass. These materials have refractive indexes which are rather higher than the ideal figure. It is nevertheless possible to reduce the reflection to less than 1% of the incident white light (Longhurst, 1973).

Example

A lens is made of crown glass (refractive index 1.52). Find the thickness and refractive index of a surface coating which will eliminate reflections from the surface of the glass at a wavelength of 0.5 μm.

Solution

Since, from (1.79), the wave impedance in a dielectric is inversely proportional to the square root of the relative permittivity it is also inversely proportional to the refractive index. The refractive index of the surface coating must be the geometric mean of the refractive indices of the glass and of free space, that is $\sqrt{1.52} = 1.23$.

The wavelength of the light in the surface layer is obtained by multiplying the free-space wavelength by the refractive index. Thus the thickness of the layer should be $(0.25 \times 0.5 \times 1.23) = 0.153\,\mu m$.

3.7 QUASI TEM WAVEGUIDES

A number of different types of two-wire TEM transmission lines were introduced in Chapter 2. Several other types of two-wire line are illustrated in Fig. 3.10. Superficially these are like the transmission lines shown in Fig. 2.1 but a little thought reveals that there are differences. The most obvious one is that the lines shown in Fig. 3.10 are not embedded in a homogeneous dielectric. Take the case of microstrip (Fig. 3.10(a)) as an example. The signal is guided by the strip conductor on the top of the dielectric substrate and the ground plane conductor beneath it. For purposes of analysis the region above the ground plane can be divided into two parts: the region within the substrate and the whole of the air space above it. In each of these regions the propagating waves must satisfy Maxwell's equations. If we suppose that this line carries a TEM wave like the lines discussed in Chapter 2 then the phase velocity of the parts of the wave within the two regions will differ from each other. In other words the wave in the air would travel faster than that in the dielectric and get out of step with it. If that were to happen the fields would no longer satisfy the boundary conditions at the interface between the two regions. We conclude, therefore, that a microstrip line cannot propagate a pure TEM wave. A similar argument can be applied to each of the other lines shown in Fig. 3.10.

Microstrip is much the commonest of the three types of line shown in Fig. 3.10. It is used extensively in the hybrid and monolithic integrated

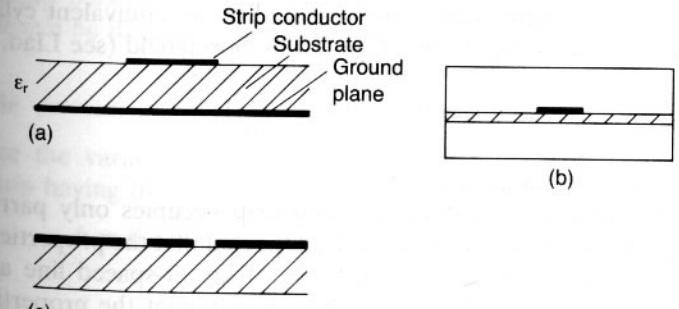

Fig. 3.10 Quasi-TEM transmission lines: (a) microstrip, (b) suspended substrate stripline and (c) coplanar waveguide.

circuits which are used for all low-power microwave signal processing. Suspended stripline has the advantage of low loss and it is used to make microwave filters whilst the balanced arrangement of coplanar waveguide is useful for the realization of balanced mixer circuits (Edwards, 1981). For all three it turns out that at low frequencies (below 2 GHz in the case of microstrip) the parameters of the line can be computed to a good approximation by static analysis. For this reason these lines can be refered to as 'quasi-TEM lines'. The discussion which follows will concentrate on microstrip.

As a starting point for the theory of microstrip consider the lines shown in Fig. 3.11. The wire over a ground plane shown in Fig. 3.11(a) can be analysed by elementary techniques (Carter, 1986) to give an expression for the capacitance per unit length

$$C = \frac{2\pi\varepsilon}{\ln(4h/d)} \tag{3.28}$$

for $h \gg d$. Because this line is surrounded by a homogeneous dielectric it carries a TEM wave whose phase velocity is

$$v_p = \frac{1}{\sqrt{(\varepsilon\mu)}} = \frac{1}{\sqrt{(LC)}}, \tag{3.29}$$

where C and L are the capacitance and inductance per unit length. The characteristic impedance is therefore

$$Z_0 = \sqrt{\left(\frac{L}{C}\right)} = \frac{1}{2\pi}\sqrt{\left(\frac{\mu}{\varepsilon}\right)}\ln\left(\frac{4h}{d}\right). \tag{3.30}$$

The strip line over a ground plane shown in Fig. 3.11(b) is likewise surrounded by a uniform dielectric and therefore supports a TEM wave. This arrangement is not readily analysed by analytical methods but its resemblance to that of Fig. 3.11(a) suggests that it might be possible to find an empirical relationship between the dimensions of the two systems so that the strip conductor can be represented by an equivalent cylindrical wire. Such a formula has been suggested by Springfield (see Liao, 1980)

$$d = 0.67w\left(0.8 + \frac{t}{w}\right), \tag{3.31}$$

where t/w is in the range 0.1 to 0.8.

Since the dielectric substrate of microstrip occupies only part of the space around the conductors it might be expected that the properties of the line would lie somewhere between those of an air-spaced line and one completely immersed in dielectric. This suggests that the properties of a microstrip line could be calculated by replacing the permittivity in (3.30) by an effective permittivity. A formula for this purpose has been suggested by Di Giacomo (1958)

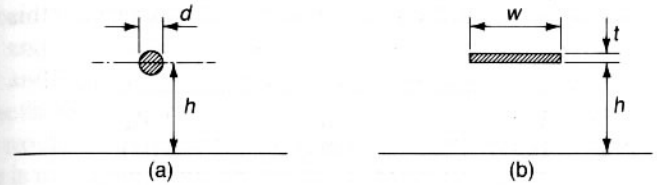

Fig. 3.11 Dimensions for lines over ground planes: (a) thin wire and (b) strip conductors.

$$\varepsilon_{re} = 0.475\varepsilon_r + 0.67, \tag{3.32}$$

where ε_r is the relative permittivity of the substrate material and ε_{re} is the effective relative permittivity to be used in (3.30). Combining (3.30), (3.31) and (3.32) gives an expression for the characteristic impedance of a microstrip line whose width is less than the substrate thickness

$$Z_0 = \frac{377}{2\pi}\frac{1}{\sqrt{(0.475\varepsilon_r + 0.67)}}\ln\left(\frac{5.97h}{0.8w + t}\right). \tag{3.33}$$

This formula gives useful results up to a ratio w/h of 0.8.

For the extreme case of a line whose width is large compared with the thickness of the substrate it is possible to neglect the fringing fields so that the capacitance per unit length is just

$$C = \varepsilon w/h, \tag{3.34}$$

which gives

$$Z_0 = \frac{377}{\sqrt{\varepsilon_r}}\frac{h}{w} \tag{3.35}$$

for the characteristic impedance. Note that this time the effective permittivity is not used because of the assumption implicit in (3.34) that all the electric field between the conductors lies in the dielectric substrate. The relationship between the two formulae given for the characteristic impedance can be illustrated by considering an example.

Example

Estimate the variation of characteristic impedance with line width for microstrip having the following parameters

$$h = 0.5\,\text{mm},\ t = 0.05\,\text{mm},\ \varepsilon_r = 9.6\ \text{(alumina)}.$$

Solution

For narrow linewidths we use (3.30), (3.31) and (3.32). From (3.32) the effective value of the relative permittivity is 5.23. The values of d and Z_0

may then be computed for the range of values of w for which this approximation is valid.

w (mm)	d (mm)	Z_0 (Ω)
0.1	0.087	82.1
0.2	0.141	69.5
0.3	0.194	61.1
0.4	0.248	54.7

For broad lines (3.35) is employed. The smallest value of w for which it is reasonable to suppose that the formula is valid is 2.0 mm. Computations for this and larger values of w yield the following.

w (mm)	Z_0 (Ω)
2.0	30.4
2.5	24.3
3.0	20.3

These figures are plotted in Fig. 3.12. The line has been sketched in so that it is asymptotic to the two curves as $w \rightarrow$ zero and $w \rightarrow$ infinity. From this it seems that the error in (3.33) is about 10% at worst for $w/h < 0.8$. Formula (3.35) is apparently valid to the same accuracy for $w/h > 3.0$. The curve may be expected to give values correct to within 10% in the region where neither formula is valid. Thus a 50 Ω line should have a width of around 0.8 mm which value is accurate enough for preliminary design calculations. The range of impedance values shown in this example is very typical of those normally used in microstrip circuits.

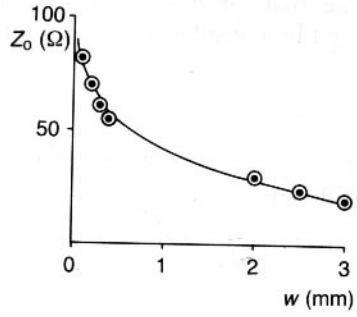

Fig. 3.12 Variation of characteristic impedance with strip width for a microstrip transmission line.

The preceding example has been included to show how the formulae can be used and what their limitations are. Methods of this kind involving effective and equivalent values are very commonly used to provide simple design methods for a whole range of complex problems where a full field solution would be too slow or difficult. An important application of these formulae is in computer-aided design (CAD) packages. A number of CAD packages are in common use for microstrip circuit design and these make use of formulae which are more complicated than those discussed above but which have been derived by very similar arguments. In particular these formulae make use of expressions for the effective permittivity which are frequency dependent to allow for the facts that the mode propagated is not a true TEM mode and that the line is therefore dispersive. Full details can be found in Edwards (1981) and Getsinger (1973).

Finally, it is important to remember that, like all other transmission lines, microstrip can propagate higher-order modes. These modes, which are cut off within the normal frequency band of the microstrip, set an upper limit on the frequency for which it can be used and also produce reactive parasitic effects at discontinuities in the line. This subject is discussed further in Chapter 6.

3.8 NON-TEM WAVEGUIDES

Besides the quasi TEM waveguides discussed in the previous section a number of other guides are sometimes employed in low power microwave circuits. These are shown in Fig. 3.13.

Slot line is the dual of an isolated strip line. It is useful when it is necessary to include shunt components in a circuit. The range of characteristic impedances which can be achieved is 60 to 200 Ω but the loss is rather high. An important use of slot line is in slot antennas. These are discussed in Chapter 5.

Fin line is superficially like the ridge waveguides discussed in Chapter 2. The range of impedances which can be realized is wide (10 to 400 Ω) and the losses are low.

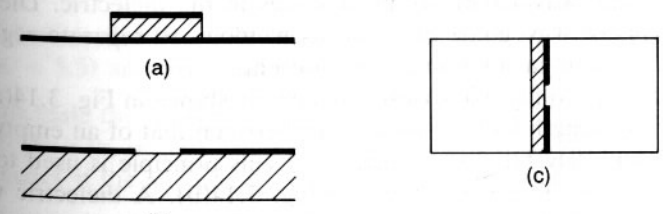

Fig. 3.13 Non-TEM waveguides: (a) image line, (b) slot line and (c) fin line.

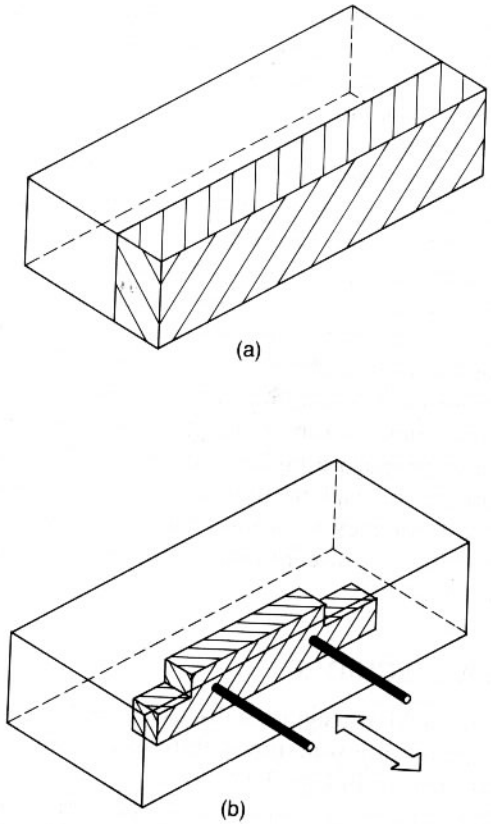

Fig. 3.14 (a) Rectangular waveguide partially filled with a dielectric material. (b) A waveguide moving vane phase changer.

Image line resembles dielectric waveguide. It can be made with very low loss and finds its applications at frequencies above 100 GHz.

The properties of rectangular and circular waveguides can be modified by the addition of dielectric materials. Thus, if a rectangular waveguide is filled with a dielectric material the free-space wavelength λ_0 in (2.35) is replaced by the wavelength of TEM waves in the dielectric. Dielectric-filled sections of waveguide are used as windows to separate regions of guide in which the gas pressures are different.

If a guide is partially filled with dielectric as shown in Fig. 3.14(a) then the guide wavelength will lie somewhere between that of an empty guide and one completely filled with dielectric. This principle is used to make waveguide phase-shifters as shown in Fig. 3.14(b). A dielectric vane is arranged so that it can be moved across the guide from the region of weak electric field near the wall to the strong field at the centre. The ends of the vane are stepped or tapered to ensure a satisfactory match. The effect of the vane is to modify the shunt capacitance of the guide (see Fig. 2.18) and, hence, its cut-off frequency (2.53). The device therefore acts as a variable phase shifter. The phase shift varies with frequency because the length of the vane in wavelengths is frequency dependent. An alternative form of phase shifter (Fox, 1947) uses a circular waveguide and a vane which rotates about the axis of the guide rather like the rotary vane attenuator described in Section 4.6.

3.9 CONCLUSION

In this chapter we have considered the reflection and refraction of waves at the boundaries between dielectric materials. The reflection of waves has been shown to depend upon their polarization, a phenomenon which is employed in the windows of gas lasers. Consideration of the circumstances in which waves can be trapped within dielectric strips and rods led on to a discussion of the properties of dielectric and optical fibre waveguides. The advantages of single-mode and multi-mode fibres were explored.

Consideration of the reflection of waves at multiple boundaries such as those encountered in radomes and microwave windows led to an understanding of the principles underlying the design of these components. In the optical field the same approach is used to minimize the reflections from the surfaces of lenses and other optical components.

Finally a number of waveguides incorporating inhomogeneous dielectrics were discussed. These guides, especially microstrip, are of considerable practical importance but are not easily analysed. The development of design formulae for microstrip was used to illustrate the kinds of methods which are commonly employed.

EXERCISES

3.1 Calculate the critical angle for total internal reflection for epoxy resin ($\varepsilon_r = 3.5$).

3.2 Calculate the relative permittivity of water at optical wavelengths given that the critical angle is 49°.

3.3 Calculate the Brewster angle for soda glass ($\varepsilon_r = 6.1$), epoxy resin ($\varepsilon_r = 3.5$) and perspex ($\varepsilon_r = 2.6$).

3.4 Calculate the cut-off frequencies for the lowest TE mode in a sheet of alumina ($\varepsilon_r = 8.9$) 1 mm thick. What would be the new cut-off frequency if the alumina were potted in epoxy resin ($\varepsilon_r = 3.5$)?

3.5 A radome made of glass-reinforced plastic having a relative permittivity of 4.5 is designed for use at 5 GHz. Calculate the minimum

thickness which can be used and the reflection coefficients at 4.5 GHz and 5.5 GHz.

3.6 It is proposed that the broadband reflection coefficient of the radome in the previous question should be improved by coating it on both sides with perspex ($\varepsilon_r = 2.6$). Suggest a suitable thickness of perspex and calculate the new reflection coefficients at 4.5 and 5.5 GHz.

3.7 Calculate the dimensions of microstrip lines having conductors 0.05 mm thick and fused quartz substrate ($\varepsilon_r = 3.8$) which have characteristic impedances of 25, 50 and 100 Ω.